Clim. Past Discuss., 6, 1701–1731, 2010
www.clim-past-discuss.net/6/1701/2010/
doi:10.5194/cpd-6-1701-2010


Climate of the Past Discussions



# Southern Ocean warming and hydrological change during the Paleocene–Eocene thermal maximum

**A. Sluijs[1], P. K. Bijl[1], S. Schouten[2], U. Röhl[3], G.-J. Reichart[4], and H. Brinkhuis[1]**

[1]Biomarine Sciences, Institute of Environmental Biology, Utrecht University, Laboratory of Palaeobotany and Palynology, Budapestlaan 4, 3584 CD Utrecht, The Netherlands
[2]Royal Netherlands Institute for Sea Research (NIOZ), Department of Marine Organic Biogeochemistry, P.O. Box 59, 1790 AB, Den Burg, Texel, The Netherlands
[3]Marum – Center for Marine Environmental Sciences, University of Bremen, Leobener Strasse, 28359 Bremen, Germany
[4]Department of Earth Sciences, Utrecht University, Budapestlaan 4, 3584 CD Utrecht, The Netherlands

Received: 9 August 2010 – Accepted: 20 August 2010 – Published: 8 September 2010

Correspondence to: A. Sluijs (a.sluijs@uu.nl)

Published by Copernicus Publications on behalf of the European Geosciences Union.







## Abstract

A brief (~150 kyr) period of widespread global average surface warming marks the transition between the Paleocene and Eocene epochs, ~56 million years ago. This so-called "Paleocene–Eocene thermal maximum" (PETM) is associated with the massive injection of $^{13}C$-depleted $CO_2$ and/or $CH_4$, reflected in a negative carbon isotope excursion (CIE). Biotic responses include a global dominance (acme) of the subtropical dinoflagellate *Apectodinium*. Here we identify the PETM in a marine sedimentary sequence deposited on the East Tasman Plateau at Ocean Drilling Program (ODP) Site 1172 and show that Southwest Pacific sea surface temperatures increased from ~26 °C to ~33 °C during the PETM. Such temperatures before, during and after the PETM are >10 °C warmer than predicted by paleoclimate model simulations for this latitude, suggesting that not only Arctic, but also Antarctic temperatures are underestimated in simulations of ancient greenhouse climates by current generation fully-coupled climate models. An early influx of abundant *Apectodinium* confirms that environmental change preceded the CIE on a global scale. Organic dinoflagellate cyst assemblages suggest a local decrease in the amount of river run off reaching the core site during the PETM, possibly in concert with eustatic rise. Moreover, the assemblages suggest changes in seasonality of the regional hydrological system and storm activity. Finally, significant variation in dinoflagellate cyst assemblages during the PETM indicates that the Southwest Pacific climate state was more dynamic during this event than before and after, a finding comparable to similar studies of PETM successions from the New Jersey Shelf.

## 1 Introduction

Gradual global warming initiated in the late Paleocene (~59 Ma) and culminated in the Early Eocene Climatic Optimum (EECO; 52–50 Ma) (e.g., Zachos et al., 2001; Bijl et al., 2009). Superimposed on this long-term warming trend, at least four "hyperthermals" occurred, i.e. relatively brief (<200 kyr) intervals characterized by anomalously





CPD
6, 1701–1731, 2010



high temperatures (e.g., Bowen et al., 2006; Sluijs et al., 2007a). These include the Paleocene–Eocene Thermal Maximum (Kennett and Stott, 1991; Zachos et al., 1993) (PETM; ∼56 Ma), Eocene Thermal Maximum 2 (ETM2; ∼54 Ma) (Lourens et al., 2005), H2 (100 kyr younger than ETM2, Cramer et al., 2003; Stap et al., 2010) and the informally-termed "X" event (∼53 Ma) (Röhl et al., 2005; Agnini et al., 2009). The PETM is the most prominent and best studied hyperthermal and is marked by a negative carbon isotope excursion (CIE) in sedimentary components of 2.5–8‰, depending on analyzed substrate, location and completeness of the section (Kennett and Stott, 1991; Koch et al., 1992; Schouten et al., 2007b; Handley et al., 2008; McCarren et al., 2009). These records are consistent with geologically rapid, massive injections of $^{13}$C-depleted carbon into the ocean-atmosphere system (Dickens et al., 1997; Higgins and Schrag, 2006; Panchuk et al., 2008; Zeebe et al., 2009), although the mechanism for such release remains controversial (Dickens et al., 1995; Kurtz et al., 2003; Svensen et al., 2004; Higgins and Schrag, 2006).

Traditional stable oxygen isotope ($\delta^{18}$O) and Mg/Ca studies on planktonic foraminifera from deep-sea sediments indicate a 5–8 °C surface warming during the PETM (Kennett and Stott, 1991; Thomas et al., 2002; Zachos et al., 2003). Reconstruction of absolute sea surface temperatures (SST) from such sections has been problematic because of post-sedimentary recristallization of planktonic foraminifera (Schrag et al., 1995; Pearson et al., 2001). Additionally, reduced pH may have dampened foraminifer $\delta^{18}$O excursions, potentially resulting in too low estimates of PETM warming (Uchikawa and Zeebe, 2010). More recently, the application of organic paleothermometers, such as $TEX_{86}$ and MBT/CBT in marginal marine sequences provided estimates of absolute temperature evolution across the PETM and other hyperthermals in the Northern Hemisphere (e.g., Sluijs et al., 2006; Zachos et al., 2006; Weijers et al., 2007). These studies showed exceptionally high Arctic temperatures during this time interval, suggesting very low meridional temperature gradients (Sluijs et al., 2006). The marginal marine sections used in these studies have also revealed significant increases in river discharge and sediment input (e.g., Crouch et al., 2003; Giusberti et





CPD
6, 1701–1731, 2010



al., 2007; John et al., 2008; Sluijs et al., 2008b; see also overview in Sluijs et al., 2008a), changes in trophic level (e.g., Crouch et al., 2001; Speijer and Wagner, 2002; Gibbs et al., 2006), as well as eustatic rise (Sluijs et al., 2008a). However, temperature and paleoecological data from marginal marine PETM sections from the Southern Hemisphere are rare (Crouch et al., 2001; Crouch and Brinkhuis, 2005), and none are available from the Southern Ocean, hampering thorough evaluation of climatic change in the sub-Antarctic realm.

We have generated geochemical and palynological data through upper Paleocene–lower Eocene sediments recovered during Ocean Drilling Program (ODP) Leg 189 at Site 1172 on the East Tasman Plateau, deposited at ~65° S paleolatitude (Exon et al., 2004) (Fig. 1). Micropaleontological information from the Southwest Pacific showed that this site was located within the Antarctic-derived, northward flowing Tasman Current throughout the Paleogene, which is consistent with general circulation model experiments (Huber et al., 2004). While in an earlier study, based on initial shipboard samples we suggested that the PETM might not have been recovered at this site (Röhl et al., 2004), detailed post-cruise investigations identified a condensed PETM section, on the basis of the CIE. We perform $TEX_{86}$, dinoflagellate cyst assemblage analyses and X-ray fluorescence (XRF) core scanning, in order to reconstruct paleoenvironmental conditions at southern high latitudes across the PETM.

## 2 Material and methods

### 2.1 Material

Sediments of late Paleocene and early Eocene age at Site 1172, Hole 1172D, consist mainly of organic-rich green and gray clay- and siltstones with low abundance of calcareous and siliceous microfossils, but high abundance of palynomorphs (notably dinocysts but also terrestrial pollen and spores). Glauconite and accessory minerals are recorded in varying abundance (Shipboard Scientific Party, 2001), with





CPD
6, 1701–1731, 2010



the glauconite grains being irregular and angular, which indicates that glauconite was formed in situ (based on thin sections, not shown). Lithological and palynological information, as well as the general absence of calcareous microfossils, suggests an overall very shallow marine depositional setting, to restricted conditions with marked runoff from the nearby shores (Shipboard Scientific Party, 2001; Röhl et al., 2004).

Integrated dinoflagellate cyst and magnetostratigraphic studies identified Chrons C25n, C24r and C24n, with the top of Chron C25n at 618.00 rmbsf and the onset of Chron C24n at 594.2 rmbsf (Fuller and Touchard, 2004; Stickley et al., 2004; Bijl et al., 2009). Average sedimentation rates implied by this age model are 5.7 m/Myr, when assuming a duration of 3.1 Ma for Chron C24r (Westerhold et al., 2007).

### 2.2 Methods

The archive halves of Core 189-1172D-15R were subject to XRF Core Scanning. Subsequently, half-splits of these archive halves were sampled on a resolution of 1 to 2 cm, after which samples were freeze-dried. Splits of samples were then taken for palynology and organic geochemistry.

#### 2.2.1 X-ray fluorescence (XRF) core scanning

We measured the elemental composition of sediments from Cores ODP 189-1172D-15R to -17R at the MARUM, Bremen University, Germany, using the XRF core scanner (Richter et al., 2006; Tjallingii et al., 2007). The XRF core scanner acquires bulk-sediment chemical data from split core surfaces. Although measured elemental intensities are predominantly proportional to concentration, they are also influenced by the energy level of the X-ray source, count time, and physical properties of the sediment (Röhl and Abrams, 2000; Tjallingii et al., 2007). XRF data were collected every cm down-core over a 1 $cm^2$ area using 30 s count time. We used a generator setting of 20 kV and an X-ray current of 0.15 mA.





CPD
6, 1701–1731, 2010



### 2.2.2 Palynology

Samples of 1–2 cm stratigraphic thickness were freeze-dried and a known amount of *Lycopodium* spores was added to ~4 g of material. Samples were then treated with 30% HCl and twice with 38% HF for carbonate and silicate removal, respectively. Residues were sieved using a 15-µm nylon mesh to remove small particles. To break up clumps of residue, the sample was placed in an ultrasonic bath for a maximum of 5 min, sieved again, and subsequently concentrated into 1 ml of glycerine water, of which 10 µl was mounted on microscope slides. Slides were counted for marine (e.g., dinocysts) and terrestrial palynomorphs (e.g., pollen and spores) to a minimum of 200 dinocysts. Marine and terrestrial palynomorph preservation was excellent for all samples. We generally follow dinocyst taxonomy of Fensome and Williams (2004), but adapt Sluijs et al. (2009a) for the various spiny peridinioid taxa. Absolute quantitative numbers were counted using the relative abundance of *Lycopodium* spores (cf., Stockmarr, 1972).

### 2.2.3 Organic geochemistry

For stable carbon isotope analyses of total organic carbon ($\delta^{13}C_{TOC}$), freeze-dried samples were powdered, treated with 1 M HCl to remove carbonate, centrifuged and the supernatant decanted, followed by two rinses with demineralized water and freeze-dried again. Residues were analyzed with a Fison NA 1500 CNS analyzer coupled to a Finnigan Delta Plus isotope ration mass spectrometer. Analytical precision and accuracy were determined by replicate analyses and by comparison with in-house standards, and were better than 0.1‰ and 0.1‰, respectively.

For biomarker analyses, freeze-dried sediment samples (~3.5 g dry mass) were extracted with dichloromethane (DCM)/methanol (2:1) using accelerated solvent extraction (Dionex ACE). The extracts were separated by $Al_2O_3$ column chromatography using hexane/DCM (9:1, v/v) and DCM/methanol (1:1, v/v) to yield the apolar and polar fractions, respectively. The polar fractions were analyzed using high performance





CPD
6, 1701–1731, 2010



liquid chromatography/atmospheric pressure chemical ionization-mass spectrometry, according to Schouten et al. (2007a). Single ion monitoring was used to quantify the abundance of the crenarchaeotal Glycerol Dialkyl Glycerol Tetraether (GDGT) lipids. The relative abundance of GDGTs were used to calculate $TEX_{86}$ (Schouten et al., 2002). $TEX_{86}$ is converted to mean annual SST by means of quasi-global core top calibrations. A new calibration with a logarithmic function was recently published (Kim et al., 2010), which is based on the currently available core-top data and a thorough statistical analyses between GDGTs abundances and SST. An earlier calibration assumes a different logarithmic relation (Liu et al., 2009) that produces particularly different SSTs for high $TEX_{86}$ values. We also determined the BIT index, which is a ratio between soil bacteria-derived and marine crenarchaeota-derived membrane lipids, a proxy for the amount of river transported soil organic matter versus marine organic matter (Hopmans et al., 2004).

#### 2.2.4 Core depth adjustments

Based on correlations between physical properties data generated on core material and downhole logging, we have slightly changed the meters below sea floor (mbsf) depth of the core sediments (Bijl et al., 2009); we use revised mbsf (rmbsf) for these revised depths throughout. Relative to mbsf, Core 189-1172D-12R was shifted up by 0.36 m; 13R down by 1.87 m; 14R down by 2.84 m; 15R down by 2.4 m; 16R down by 2.57 m and 17R down by 2.66 m.

## 3 Results

### 3.1 Stratigraphy

Between 611.89 and 611.86 rmbsf, the $\delta^{13}C_{TOC}$ curve shows a ~3‰ negative step from −26 to −29‰, followed by a ~20 cm interval of relatively stable values, and a subsequent exponential recovery that reaches background values between 611.2 and





CPD
6, 1701–1731, 2010



611.0 rmbsf (Fig. 2). This excursion is located within magnetochron C24r. Average sedimentation rates of 5.7 m/Myrs for this chron (see Material) imply that this excursion occurred ~1 Ma after the termination of Chron C25n (Fuller and Touchard, 2004; Bijl et al., 2009) and ~2 Ma between this CIE and the onset of Chron C24n. The orbitally based age model from Blake Nose (ODP Leg 171B) and Walvis Ridge (ODP Leg 208) also indicates ~1 Ma between the top of Chron C25n and the PETM (Norris and Röhl, 1999), and ~2 Ma between the PETM and the onset of Chron C24n (Westerhold et al., 2007). Hence, the overall stratigraphic position of the CIE implies the presence of the PETM in Core 1172D-15R. The thickness of the CIE at Site 1172 is 65–90 cm, depending on the definition of its termination (Röhl et al., 2007). Assuming a 170 kyr duration of the CIE (Röhl et al., 2007; Abdul Aziz et al., 2008), this indicates average PETM sedimentation rates of ~0.4–0.5 cm/kyr, although sediment accumulation rates were likely highly variable in this pro-deltaic setting.

### 3.2 $TEX_{86}$ and BIT

Late Paleocene SSTs average ~26 °C ($1\sigma$=0.9) based on $TEX_{86}$, regardless of the applied calibration (Fig. 2). Concomitantly with the onset of the CIE, SSTs rise to average PETM values of ~31 °C ($1\sigma$=0.7) following KIM2010, or ~29 °C for LIU2009 with peak values of almost 33 °C and 31 °C for the two calibrations, respectively, at 611.70 rmbsf. The magnitude of PETM warming was thus ~7 °C with KIM2010 and 4 °C with LIU2009. SSTs returned to pre-excursion values during the recovery of the CIE. The warming and the CIE are preceded by two samples with relatively low temperatures (~25 °C).

BIT values are low throughout the analyzed interval, indicating that $TEX_{86}$ values are not influenced by soil derived GDGTs (Weijers et al., 2006). The BIT record exhibits some scatter, but values during the PETM (0.09±0.02) are on average somewhat lower than before and after the PETM (0.13±0.03), suggesting increased marine production of GDGTs or a decreased supply of soil organic matter.





CPD
6, 1701–1731, 2010



### 3.3 Palynology

Palynological assemblages are rich, well preserved and dominated by dinoflagellate cysts (dinocysts). Terrestrial pollen and spores are common to abundant throughout, with relatively high abundances within the PETM (Figs. 2, 3). Stratigraphically important dinocyst taxa include *Apectodinium* spp., *Eocladopyxis peniculatum*, *Deflandrea* spp., *Melitasphaeridium pseudorecurvatum, Muratodinium fimbriatum* and the recently described species *Florentinia reichartii*. (Sluijs and Brinkhuis, 2009). In particular the oldest abundant occurrence (>40% of the assemblage) of *Apectodinium* in the Southwest Pacific Ocean has been calibrated to the PETM (Crouch, 2001). At Site 1172, however, the First Occurrence (FO) of abundant *Apectodinium* is at ~612.6 rmbsf, ~75 cm below the onset of the CIE (Fig. 3). *Apectodinium* abundances subsequently decrease to ~2%, followed by a second abundance maximum starting at the onset of the CIE.

Along with *Apectodinium* spp., other quantitatively significant taxa in the assemblage mostly comprise cosmopolitan taxa such as *Senegalinium* spp., *Glaphyrocysta* spp., *Eocladopyxis peniculatum*, *Cordosphaeridium fibrospinosum*, *Thalassiphora* spp., *Kenleyia* spp., *Fibrocysta* spp. (and other members of the *Cordosphaeridium fibrospinosum* complex) (sensu, Sluijs and Brinkhuis, 2009), *Diphyes colligerum, Paucisphaeridium, Deflandrea* (and a few related *Cerodinium*), *Membranosphaera* (often referred to as *Elytrocysta* in the Southern Ocean), and *Spiniferites* spp. *Hystrichosphaeridium truswelliae*, common in certain intervals, was long thought to have been endemic to the Antarctic Realm, but was recently recorded in uppermost Paleocene and PETM sediments on the New Jersey Shelf (Sluijs and Brinkhuis, 2009). In fact, PETM assemblages as a whole are strikingly similar to those reported from the New Jersey Shelf. Only few aspects of the assemblages are typical for the Antarctic Realm (e.g., Wrenn and Beckmann, 1982; Warnaar et al., 2009), including rare *Vozzhennikovia* spp., and temporally abundant *Pyxidinopsis* spp.





CPD
6, 1701–1731, 2010



*Senegalinium* spp. dominate assemblages from the base of the studied section (~615 rmbsf) up to ~613 rmbsf, an interval with very stable dinocyst assemblages with common *Pyxidinopsis*, *Spiniferites*, and *Deflandrea* spp. Assemblages are slightly richer above ~613 rmbsf, with more abundant *Pyxidinopsis* spp. and common *H. truswelliae* and *Membranosphaera* spp. A peak in *Glaphyrocysta* spp. occurs around 613 rmbsf, directly followed by the first *Apectodinium* acme. Between 612.2 and 611.9 rmbsf, just below the onset of the CIE, successive transient abundances of *Glaphyrocysta*, *Deflandrea*, *Pyxidinopsis*, and *Operculodinium* spp., and *C. fibrospinosum* complex occur. A second acme of *Apectodinium* is recorded concomitant with the CIE. Within the CIE, transient abundances of *Glaphyrocysta* spp. and *Eocladopyxis peniculatum* occur. After the CIE, *Senegalinium* dominates assemblages again, while *Operculodinium* spp., *H. truswelliae* and *Membranosphaera* spp. are common.

### 3.4 XRF

We present high-resolution XRF core scanner data for Core 1172A-15R across the carbon isotope excursion (CIE) of the PETM (Fig. 2). Fe and Ca intensities exhibit a characteristic variability that can be directly attributed to lithology (Fig. 2). The Ca in these sediments is related to carbonate (Röhl et al., 2004). The dominant lithology, organic-rich green and gray clay- and siltstones with low carbonate contents (Shipboard Scientific Party, 2001) is expressed as generally low Ca values in cores below Core 15R (Röhl et al., 2004). Ca values are higher in the lower part of Core 15R, just below the PETM (Fig. 2). The Ca intensities in this interval of Core 15R show regular fluctuations: about four cycles below the onset of the PETM, which are also visible in the BIT index, the $TEX_{86}$ sea surface temperature data, and reversely in the percentage of terrestrial palynomorphs. Assuming an average sedimentation rate of 5.7 m/Myr these cycles could represent the low eccentricity frequency of the Milankovitch orbital band (100 kyr cycles). Ca values exhibit a peak during the warming of the PETM, followed by the lowest Ca values in the interval (611.56–610.57 rmbsf) (Fig. 2). The Fe





CPD
6, 1701–1731, 2010



and Ca intensities are overall anti-correlated. The Fe record exhibits maximum values (broad peak) in the upper part of the CIE, where the Ca values are low and the terrestrial palynomorphs show maximum values.

## 4 Discussion

### 4.1 The carbon isotope excursion

The ~3‰ CIE recorded at Site 1172 is slightly smaller in amplitude than the 4–5‰ often recorded in $\delta^{13}C_{TOC}$ at other marine sites (Bolle et al., 2000; Steurbaut et al., 2003; Sluijs et al., 2006). Since the lowest $\delta^{13}C$ values for most carbon isotope records across the PETM are located close to the onset of the event (e.g., Bowen et al., 2001; Thomas et al., 2002; Sluijs et al., 2007a), this could imply that the earliest part of the PETM is not represented in our record. However, globally, $\delta^{13}C$ curves from the PETM indicate a rapid decrease (<10 000 yr), followed by ~80 kyr of stable carbon isotope values and subsequent recovery, often referred to as the "body" of the CIE (e.g., Thomas and Shackleton, 1996; Bowen et al., 2001; Thomas et al., 2002; Sluijs et al., 2007a; McCarren et al., 2009). Our record clearly shows an interval of stable values of around −29‰ between ~611.9–611.7 rmbsf, implying that at least part of the stable peak phase is represented in the record. In fact, the magnitude of the CIE in our record is very close to the −3 to −3.5‰ that is generally assumed to have been the excursion in the global exogenic carbon (Zachos et al., 2007; McCarren et al., 2009). Hence, the record at Site 1172 appears to contain at least part of the "body" of the CIE as well as the recovery, allowing comparison to other PETM sites.

### 4.2 Sea surface temperature evolution

The range of SST estimates based on $TEX_{86}$ is large due to differences in calibrations; LIU2009 gives relatively low temperature estimates and implies a very low sensitivity





CPD
6, 1701–1731, 2010



for $TEX_{86}$ values at temperatures >30 °C. In contrast, KIM2010 implies a higher sensitivity and absolute temperature estimates (Fig. 2). In the New Jersey PETM records for example, the KIM2010 is most consistent with mixed layer planktonic foraminifer stable oxygen isotope ($\delta^{18}O$) paleothermometry (Kim et al., 2010), also regarding the magnitude of warming. In this upper range of $TEX_{86}$ values, we therefore prefer the magnitude of warming implied by the KIM2010 calibration.

A warming of ~7 °C is similar to or slightly less than the only other Southern Ocean estimates from the Weddell Sea (Sites 689 and 690 at Maud Rise), based on the $\delta^{18}O$ excursion in the surface dwelling foraminifer *Acarinina* (Thomas et al., 2002; Zachos et al., 2007). The magnitude of the SST rise is also similar to that recorded at marginal marine sites on the New Jersey Shelf based on foraminiferal $\delta^{18}O$ and $TEX_{86}$ (Zachos et al., 2006; Sluijs et al., 2007b; John et al., 2008). However, the magnitude of warming was smaller in open-ocean and continental settings, and in the Arctic (e.g., Thomas and Shackleton, 1996; Zachos et al., 2003; Tripati and Elderfield, 2005; Wing et al., 2005; Sluijs et al., 2006; Weijers et al., 2007). This suggests that, while the Arctic warmed with a magnitude comparable to the global average (Sluijs et al., 2006), some marginal marine regions warmed slightly more and some polar amplification may have occurred in the Southern Hemisphere. If so, this amplification may have been caused by three mechanisms. First, the melting of small ice sheets on high mountains in Antarctica may have reduced albedo and thus amplified Antarctic warming. This would be consistent with the reconstructed PETM eustatic rise (Sluijs et al., 2008a). Secondly, an increase in atmospheric heat transport may have occurred. Indeed, increased precipitation in Southern Hemisphere PETM records would suggest more latent heat transport from tropical regions to the Antarctic (Robert and Kennett, 1994; Crouch et al., 2003). However, also Arctic sections exhibit evidence for intensified regional hydrology (Pagani et al., 2006), but no amplification of warming is recorded there (Sluijs et al., 2006). Third, a change in ocean circulation during the PETM resulted in regionally enhanced warming in the Southwest Pacific and Weddell Sea.

Absolute $TEX_{86}$ temperatures are surprisingly high for this latitude, even with the





CPD
6, 1701–1731, 2010



conservative LIU2009. Pre-PETM SSTs of ~26–27 °C and PETM SSTs of ~30–34 °C are approximately 3–6 °C cooler than on the New Jersey Shelf at a paleolatitude of ~35–40° N (Zachos et al., 2006; Sluijs et al., 2007b), and ~8–12 °C warmer than those in the Arctic (Sluijs et al., 2006) depending on the applied calibration. Post-PETM SSTs are ~5 °C lower than earliest Eocene estimates from Tanzania at ~17° S (Pearson et al., 2007). Although no $TEX_{86}$ information is available from equatorial regions for this time period, this supports previous observations (Bijl et al., 2009; Hollis et al., 2009) of a significantly reduced temperature gradient between the Southwest Pacific and at least the subtropics. As indicated for the Northern Hemisphere data (Sluijs et al., 2006, 2007b; Zachos et al., 2006), the difference in SST of merely 10 °C between Tanzania, New Zealand and Site 1172 cannot be simulated by current-generation fully coupled models (Shellito et al., 2003; Huber and Nof, 2006). However, oxygen isotopes of reputedly Eocene mollusks from coastal Antarctica indicate significantly cooler conditions on the Antarctic shelf (Ivany et al., 2008). This either implies that a very large temperature difference existed between the East Tasman Plateau and coastal Antarctica, or that $TEX_{86}$ and mollusk $\delta^{18}O$ yield significantly different paleotemperature estimates.

Interestingly, regardless of the calibration, peak PETM temperatures are similar to those recorded for the Early Eocene Climatic Optimum (EECO, ~52–50 Ma) at Site 1172 (Bijl et al., 2009). This suggests that atmospheric greenhouse gas levels were comparable during the peak of the PETM and long-term warmth of the EECO. In fact, although regional differences exist, peak PETM temperatures were similar to those during ETM2 (Sluijs et al., 2009b; Stap et al., 2010). If so, one may speculate that the long-term late Paleocene–early Eocene warming trend that culminated in the EECO as well as the superimposed hyperthermals, were caused by carbon injection from the same reservoir. Such a scenario requires a source that slowly added carbon to the global exogenic pool during the long-term trend resulting in the EECO. During the hyperthermals, it must have released carbon catastrophically, perhaps when an orbital (Lourens et al., 2005) threshold was surpassed, followed by partial recharge. One reservoir that may behave like this is the methane hydrate reservoir (Dickens, 2003).





CPD
6, 1701–1731, 2010



Although several potential problems exist with methane hydrates as the only source for $^{13}$C-depleted carbon, a long-term net leakage from hydrates during late Paleocene–early Eocene warming is consistent with a concomitant decrease in deep ocean $\delta^{13}$C as observed in benthic foraminiferal calcite.

### 4.3 Leads and lags

The genus *Apectodinium* originated close to the Danian-Selandian boundary (Brinkhuis, 1994; Guasti et al., 2006) but abundant occurrences were restricted to low latitudes until the PETM (Bujak and Brinkhuis, 1998; Iakovleva et al., 2001). On a global scale, *Apectodinium* dominates dinoflagellate assemblages described from the PETM (Heilmann-Clausen, 1985; Bujak and Brinkhuis, 1998; Egger et al., 2000; Crouch et al., 2001; Steurbaut et al., 2003; Sluijs et al., 2006, 2007a). At Site 1172, however, the lowermost acme starts approximately 70 cm below the CIE. Average sedimentation rates of 5.7 m/Myr suggest that this acme leads the CIE by some 100 kyr, although sedimentation rates likely varied significantly in this pro-deltaic setting.

An influx of abundant *Apectodinium* has also been shown to lead the CIE on the New Jersey Shelf, the Central North Sea and, perhaps, New Zealand (Sluijs et al., 2007b), by approximately 5 kyr (perhaps slightly longer if sedimentation rates decreased in response to sea level rise (see, Sluijs et al., 2008a). The early *Apectodinium* acme recorded at Site 1172 can be interpreted in two ways. First, if the uppermost Paleocene record at Site 1172 is relatively expanded, the early acme may actually correlate to the early onset recorded at other sites. Latest Paleocene sedimentation rates of ~10 cm/kyr are required to support this hypothesis, which is significantly higher than the average across this part of the section at Site 1172, but quite common for marginal marine settings. If so, the rise in $TEX_{86}$ around 612 rmbsf might comprise the warming recorded in New Jersey between the onset of the *Apectodinium* acme and the CIE (Sluijs et al., 2007b), although the latter records do not show a subsequent cooling immediately prior to the onset of the CIE. We cannot exclude this hypothesis because of the poor constraints on sedimentation rates in the uppermost Paleocene part of the





CPD
6, 1701–1731, 2010



section. Second, the early *Apectodinium* acme may imply that conditions at Site 1172 locally became similar to low latitude equatorial environments ~100 kyr prior to the CIE, but unrelated to the PETM. If so, this would imply extremely anomalous environmental change on the East Tasman Plateau, associated with the first and mass occurrence of a typical low latitude dinoflagellate in the Southern Ocean, which is not accompanied by significant change in other proxies and, critically, not recorded in nearby sections at lower latitudes in New Zealand (Crouch et al., 2001, 2003; Crouch and Brinkhuis, 2005). Although, this hypothesis seems inconsistent with the strictly low-latitude biogeography of abundant Paleocene *Apectodinium*, we cannot exclude it with the present data.

### 4.4 Depositional environment, hydrology, sea level and productivity

Low sedimentary Ca values are in line with a shallow marine depositional environment, dominated by siliciclastic input. The Ca record shows a peak during the lower part of the PETM. The persistence of carbonate accumulation in this interval indicates that the carbonate saturation state of the bottom waters at this shelf site did not drop below values that would prevent carbonate preservation, as recorded at other shelf locations (e.g., Bolle et al., 2000; John et al., 2008). Hence, the calcite saturation depth and calcite compensation depths in the deep ocean (Zachos et al., 2005), remained deeper than the shelf in the Southwest Pacific Ocean.

Representatives of the genus *Senegalinium* dominate dinocyst assemblages for most of the studied interval (Fig. 3). Dinocysts assignable to this genus have been shown to tolerate very low salinities (Brinkhuis et al., 2006). Furthermore, high *Senegalinium* abundances have been associated with salinity stratification on the New Jersey Shelf during the PETM (Sluijs and Brinkhuis, 2009). Moreover, *Senegalinium* likely represents heterotrophic dinoflagellates, thereby thriving in relatively nutrient-rich waters (Sluijs et al., 2005). Accordingly, consistent with lithological information, we interpret high abundances of *Senegalinium* spp. prior to the PETM as to indicate relatively high productive shelf settings, with sustained fresh-water runoff from





CPD
6, 1701–1731, 2010



nearby rivers. This interpretation is corroborated by relatively abundant terrestrial palynomorphs (Fig. 3). Although the low BIT values suggest a relatively low contribution of soil derived organic matter, these most likely rather reflect the high burial fluxes of marine organic matter and isoprenoid GDGTs.

A decrease in *Senegalinium* abundance at 613.3 rmbsf is accompanied by a peak in *Glaphyrocysta* spp., a taxon of which abundant occurrences are often associated with transgressive system trackts and sea level rise (Iakovleva et al., 2001; Pross and Brinkhuis, 2005), suggesting uppermost Paleocene transgression at Site 1172. Generally increasing abundances of other normal marine taxa, such as *Pyxidinopsis* spp., *C. fibrospinosum* cpx., *Spiniferites* spp., and *Operculodinium* spp. support this interpretation. A second peak in *Glaphyrocysta* spp. at the onset of the CIE also suggests renewed sea level rise during the early stages of the PETM, supported by dropping BIT index values and a second drop in *Senegalinium* abundances. This transgression is seen along continental margins on a global scale and has, hence, shown to represent eustatic rise (Sluijs et al., 2008a).

The dinocyst trends across the PETM in the Tawanui Section (New Zealand) are similar to the succession at Site 1172 (Crouch et al., 2001; Crouch and Brinkhuis, 2005). Main differences include the lower numbers of the more nearshore taxa and runoff indicators such as *Senegalinium* spp., and slightly higher numbers of more offshore taxa such as *Spiniferites* and *Impagidinium* spp. at the slope setting of Tawanui. At Tawanui, the combined proxy records where interpreted to reflect increased weathering and continental runoff (Crouch et al., 2003), while at the much more proximal Site 1172, PETM eustatic rise appears to have compensated the possible coeval runoff increase as reflected in the dinocyst assemblages.

A peak of *Eocladopyxis* spp., a member of the extant family Goniodomidae that mainly inhabits polysaline, lagoonal environments (Wall et al., 1977), occurs within the PETM. Potentially, SSTs were only warm enough for this species to thrive in the Southern Ocean during peak PETM warmth. The ecology of extant Goniodomids provides additional boundary conditions for the local environment. Abundant representatives





CPD
6, 1701–1731, 2010



of related species in the modern ocean (e.g., the harmful species *Pyrodinium bahamense*) have been related to hypersaline conditions (Reichart et al., 2004). Critically, however, in many regions, seasonal storm activity appears important to resuspend dormant cysts into the water column to hatch and fulfill their life cycle (Villanoy et al., 1996, 2006). In such systems, the subsequent bloom initiates when salinities drop due to increased river run off, and when turbulence is minimal (e.g., Dale, 2001; Siringan et al., 2008). Increased river run off and surface ocean stratification might be induced by tropical storms. Hence, storm activity and seasonal river input might have increased in the Southwest Pacific region during the PETM, consistent with increased abundances of terrestrial palynomorphs. In any case, a peak in Goniodomids has at Site 1172 only been recorded during the PETM (Fig. 3) and the EECO (Brinkhuis et al., 2003; Sluijs et al., 2003; Bijl, 2007), indicating a very particular environment for this region, likely associated with a change in seasonality of regional hydrology, maximum temperatures and perhaps storm activity.

The dinocyst record suggests relatively stable conditions through the latest Paleocene and some more variation close to the onset of the CIE and within the PETM, with short-lived abundances of *Glaphyrocysta*, *Eocladopyxis*, *Pyxidinopsis*, *Cordosphaeridium fibrospinosum* complex, *Spiniferites*, *Operculodinium*, and *Membranosphaera*. Such intra-PETM variability has also been recorded in continental deposits from Wyoming (Bowen et al., 2004; Wing et al., 2005; Kraus and Riggins, 2007) and on the New Jersey Shelf (Sluijs and Brinkhuis, 2009). Although at the moment the cause of these variations are unknown, they do suggest that climate during the PETM may have been dynamic, perhaps on a global scale.

## 5 Conclusions

A relatively complete PETM record was identified in sediments recovered from the East Tasman Plateau during ODP Leg 189, deposited at a paleolatitude of ~65° S. Sediments are almost devoid of biogenic calcite but yield rich organic microfossil





CPD
6, 1701–1731, 2010



assemblages. $TEX_{86}$ paleothermometry indicates that SSTs warmed from ~27 to 33 °C during the PETM, with a magnitude similar to or slightly larger than the global estimate of warming. Such surprisingly warm SSTs for this latitude support that meridional temperature gradients were very low across the Paleocene–Eocene transition. Maximum temperatures were similar to those during the EECO, perhaps implying similar greenhouse gas concentrations. If so, one may speculate that long-term late Paleocene to early Eocene warming, carbon isotope trends and superimposed hyperthermals, were associated with carbon release from the same reservoir, perhaps methane hydrates. The globally recorded acme of the taxon *Apectodinium* leads the CIE at Site 1172, which may represent the same early onset as recorded on the New Jersey Shelf and the North Sea. A decrease in the abundance of the fresh water-tolerant dinoflagellate cyst *Senegalinium* suggest a decrease in the influence of river run off at the core site during the PETM, possibly in concert with eustatic rise. However, a unique abundance of the euryhaline taxon *Eocladopyxis* may indicate a change in the seasonality of the regional hydrological system and an increase in storm activity. Finally, significant variation in assemblages within the PETM suggests that the climate state was relatively dynamic during this event.

*Acknowledgements.* This research used samples and data provided by the Ocean Drilling Program (ODP). Funding for this research was provided by the Netherlands Organisation for Scientific Research to AS (NWO-Veni grant 863.07.001) and SS (NWO-Vici grant), by the Deutsche Forschungsgemeinschaft (DFG) to UR, and by the LPP Foundation to PKB. We thank Arnold van Dijk, Jan van Tongeren, Natasja Welters (all Utrecht University) and Ellen Hopmans and Jort Ossebaar (Royal NIOZ) for technical support.

## References

Abdul Aziz, H., Hilgen, F. J., van Luijk, G. M., Sluijs, A., Kraus, M. J., Pares, J. M., and Gingerich, P. D.: Astronomical climate control on paleosol stacking patterns in the upper Paleocene–lower Eocene Willwood Formation, Bighorn Basin, Wyoming, Geology, 36, 531–534, doi:510.1130/G24734A.24731, 2008.





CPD
6, 1701–1731, 2010



Agnini, C., Macri, P., Backman, J., Brinkhuis, H., Fornaciari, E., Giusberti, L., Luciani, V., Rio, D., Sluijs, A., and Speranza, F.: An early Eocene carbon cycle perturbation at ~52.5 Myr in the Southern Alps: chronology and biotic response, Paleoceanography, 24, PA2209, doi:10.1029/2008PA001649, 2009.

Bijl, P. K.: Late Paleocene to early Eocene palaeo-environments in the Southwest Pacific, MSc Thesis, Department of Biology, Utrecht University, Utrecht, 97 pp., 2007.

Bijl, P. K., Schouten, S., Sluijs, A., Reichart, G.-J., Zachos, J. C., and Brinkhuis, H.: Early Palaeogene temperature evolution of the Southwest Pacific Ocean, Nature, 461, 776–779, 2009.

Bolle, M.-P., Pardo, A., Hinrichs, K.-U., Adatte, T., von Salis, K., Burns, S., Keller, G., and Muzylev, N.: The Paleocene–Eocene transition in the marginal Northeastern Tethys (Kazakhstan and Uzbekistan), Int. J. Earth Sci., 89, 390–414, 2000.

Bowen, G. J., Koch, P. L., Gingerich, P. D., Norris, R. D., Bains, S., and Corfield, R. M.: Refined isotope stratigraphy across the continental Paleocene–Eocene boundary on Polecat Bench in the Northern Bighorn Basin, in: Paleocene–Eocene Stratigraphy and Biotic Change in the Bighorn and Clarks Fork Basins, Wyoming, edited by: Gingerich, P. D., University of Michigan Papers on Paleontology 33, 73–88, 2001.

Bowen, G. J., Beerling, D. J., Koch, P. L., Zachos, J. C., and Quattlebaum, T.: A humid climate state during the Palaeocene/Eocene Thermal Maximum, Nature, 432, 495–499, 2004.

Bowen, G. J., Bralower, T. J., Delaney, M. L., Dickens, G. R., Kelly, D. C., Koch, P. L., Kump, L. R., Meng, J., Sloan, L. C., Thomas, E., Wing, S. L., and Zachos, J. C.: Eocene hyperthermal event offers insight into greenhouse warming, EOS, Transactions, American Geophysical Union, 87, 165–169, 2006.

Brinkhuis, H.: Late Eocene to early Oligocene dinoflagellate cysts from the Priabonian type-area (Northeast Italy); biostratigraphy and palaeoenvironmental interpretation, Palaeogeogr. Palaeocl., 107, 121–163, 1994.

Brinkhuis, H., Sengers, S., Sluijs, A., Warnaar, J., and Williams, G. L.: Latest Cretaceous to earliest Oligocene, and Quaternary dinoflagellate cysts from ODP Site 1172, East Tasman Plateau, in: Proceedings Ocean Drilling Program, Scientific Results, edited by: Exon, N. F., Kennett, J. P., and Malone, M., College Station, Texas, 1–48, 2003.

Brinkhuis, H., Schouten, S., Collinson, M. E., Sluijs, A., Sinninghe Damsté, J. S., Dickens, G. R., Huber, M., Cronin, T. M., Onodera, J., Takahashi, K., Bujak, J. P., Stein, R., van der Burgh, J., Eldrett, J. S., Harding, I. C., Lotter, A. F., Sangiorgi, F., van Konijnenburg-van Cittert, H., de





CPD
6, 1701–1731, 2010



Leeuw, J. W., Matthiessen, J., Backman, J., Moran, K., and The Expedition 302 Scientists: Episodic fresh surface waters in the Eocene Arctic Ocean, Nature, 441, 606–609, 2006.
Bujak, J. P. and Brinkhuis, H.: Global warming and dinocyst changes across the Paleocene/Eocene Epoch boundary, in: Late Paleocene–Early Eocene Climatic and Biotic Events in the Marine and Terrestrial Records, edited by: Aubry, M.-P., Lucas, S. G., and Berggren, W. A., Columbia University Press, New York, 277–295, 1998.
Cramer, B. S., Wright, J. D., Kent, D. V., and Aubry, M.-P.: Orbital climate forcing of $\delta^{13}C$ excursions in the late Paleocene–early Eocene (chrons C24n–C25n), Paleoceanography, 18, 1097, doi:10.1029/2003PA000909, 2003.
Crouch, E. M.: Environmental change at the time of the Paleocene–Eocene biotic turnover, Laboratory of Palaeobotany and Palynology Contribution Series, 216 pp., 2001.
Crouch, E. M., Heilmann-Clausen, C., Brinkhuis, H., Morgans, H. E. G., Rogers, K. M., Egger, H., and Schmitz, B.: Global dinoflagellate event associated with the late Paleocene thermal maximum, Geology, 29, 315–318, 2001.
Crouch, E. M., Dickens, G. R., Brinkhuis, H., Aubry, M.-P., Hollis, C. J., Rogers, K. M., and Visscher, H.: The Apectodinium acme and terrestrial discharge during the Paleocene–Eocene thermal maximum: new palynological, geochemical and calcareous nannoplankton observations at Tawanui, New Zealand, Palaeogeogr. Palaeocl., 194, 387–403, 2003.
Crouch, E. M. and Brinkhuis, H.: Environmental change across the Paleocene–Eocene transition from Eastern New Zealand: a marine palynological approach, Mar. Micropaleontol., 56, 138–160, 2005.
Dale, B.: The sedimentary record of dinoflagellate cysts: looking back into the future of phytoplankton blooms, Sci. Mar., 65, 257–272, 2001.
Dickens, G. R., O'Neil, J. R., Rea, D. K., and Owen, R. M.: Dissociation of oceanic methane hydrate as a cause of the carbon isotope excursion at the end of the Paleocene, Paleoceanography, 10, 965–971, 1995.
Dickens, G. R., Castillo, M. M., and Walker, J. C. G.: A blast of gas in the latest Paleocene: simulating first-order effects of massive dissociation of oceanic methane hydrate, Geology, 25, 259–262, 1997.
Dickens, G. R.: Rethinking the global carbon cycle with a large, dynamic and microbially mediated gas hydrate capacitor, Earth Planet. Sc. Lett., 213, 169–183, 2003.
Egger, H., Heilmann-Clausen, C., and Schmitz, B.: The Paleocene–Eocene boundary interval of a Tethyan deep-sea section and its correlation with the North Sea basin, B. Soc. Geol. Fr.,





CPD
6, 1701–1731, 2010



171, 207–216, 2000.
Fensome, R. A. and Williams, G. L.: The Lentin and Williams Index of Fossil Dinoflagellates 2004 Edition, American Association of Stratigraphic Palynologists (AASP) Contribution Series 42, 909 pp., 2004.
Fuller, M. and Touchard, J.: Magnetostratigraphy of site 1172, leg 189, in: The Cenozoic Southern Ocean: Tectonics, Sesimentation, and Climate Change Between Australia and Antarctica. Geophysical Monograph Series 151, edited by: Exon, N. F., Kennett, J. P., and Malone, M., American Geophysical Union, Washington DC, USA, 2004.
Gibbs, S. J., Bralower, T. J., Bown, P. R., Zachos, J. C., and Bybell, L. M.: Shelf and open-ocean calcareous phytoplankton assemblages across the Paleocene–Eocene thermal maximum: implications for global productivity gradients, Geology, 34, 233–236, 2006.
Giusberti, L., Rio, D., Agnini, C., Backman, J., Fornaciari, E., Tateo, F., and Oddone, M.: Mode and tempo of the Paleocene–Eocene thermal maximum in an expanded section from the Venetian pre-Alps, Geol. Soc. Am. Bull., 119, 391–412, 2007.
Guasti, E., Speijer, R. P., Brinkhuis, H., Smit, J., and Steurbaut, E.: Paleoenvironmental change at the Danian-Selandian transition in Tunisia: foraminifera, organic-walled dinoflagellate cyst and calcareous nannofossil records, Mar. Micropaleontol., 59, 210–229, 2006.
Handley, L., Pearson, P. N., McMillan, I. K., and Pancost, R. D.: Large terrestrial and marine carbon and hydrogen isotope excursions in a new Paleocene/Eocene boundary section from Tanzania, Earth Planet. Sc. Lett., 275, 17–25, 2008.
Heilmann-Clausen, C.: Dinoflagellate stratigraphy of the Uppermost Danian to Ypresian in the Viborg 1 borehole, Central Jylland, Denmark, DGU A7, 1–69, 1985.
Higgins, J. A. and Schrag, D. P.: Beyond methane: towards a theory for the Paleocene–Eocene Thermal Maximum, Earth Planet. Sc. Lett., 245, 523–537, 2006.
Hollis, C. J., Handley, L., Crouch, E. M., Morgans, H. E. G., Baker, J. A., Creech, J., Collins, K. S., Gibbs, S. J., Huber, M., Schouten, S., Zachos, J. C., and Pancost, R. D.: Tropical sea temperatures in the high-latitude South Pacific during the Eocene, Geology, 37, 99–102, 2009.
Hopmans, E. C., Weijers, J. W. H., Schefuß, E., Herfort, L., Sinninghe Damsté, J. S., and Schouten, S.: A novel proxy for terrestrial organic matter in sediments based on branched and isoprenoid tetraether lipids, Earth Planet. Sc. Lett., 224, 107–116, 2004.
Huber, M., Brinkhuis, H., Stickley, C. E., Döös, K., Sluijs, A., Warnaar, J., Schellenberg, S. A., and Williams, G. L.: Eocene circulation of the Southern Ocean: was Antarctica kept warm





CPD
6, 1701–1731, 2010



by subtropical waters?, Paleoceanography, 19, PA4062, doi:10.1029/2004PA001014, 2004.
Huber, M. and Nof, D.: The ocean circulation in the Southern Hemisphere and its climatic impacts in the Eocene, Palaeogeogr. Palaeocl., 231, 9–28, 2006.
Iakovleva, A. I., Brinkhuis, H., and Cavagnetto, C.: Late Palaeocene–early Eocene dinoflagellate cysts from the Turgay Strait, Kazakhstan; correlations across ancient seaways, Palaeogeogr. Palaeocl., 172, 243–268, 2001.
Ivany, L. C., Lohmann, K. C., Hasiuk, F., Blake, D. B., Glass, A., Aronson, R. B., and Moody, R. M.: Eocene climate record of a high southern latitude continental shelf: Seymour Island, Antarctica, Geol. Soc. Am. Bull., 120, 659–678, 2008.
John, C. M., Bohaty, S. M., Zachos, J. C., Sluijs, A., Gibbs, S. J., Brinkhuis, H., and Bralower, T. J.: North American continental margin records of the Paleocene–Eocene Thermal Maximum: Implications for global carbon and hydrological cycling, Paleoceanography, 23, PA2217, doi:10.1029/2007PA001465, 2008.
Kennett, J. P. and Stott, L. D.: Abrupt deep-sea warming, palaeoceanographic changes and benthic extinctions at the end of the Palaeocene, Nature, 353, 225–229, 1991.
Kim, J.-H., van der Meer, J., Schouten, S., Helmke, P., Willmott, V., Sangiorgi, F., Koç, N., Hopmans, E. C., and Sinninghe Damsté, J. S.: New indices and calibrations derived from the distribution of crenarchaeal isoprenoid tetraether lipids: implications for past sea surface temperature reconstructions, Geochim. Cosmochim. Ac., 74, 4639–4654, 2010.
Koch, P. L., Zachos, J. C., and Gingerich, P. D.: Correlation between isotope records in marine and continental carbon reservoirs near the Palaeocene/Eocene boundary, Nature, 358, 319–322, 1992.
Kraus, M. J. and Riggins, S.: Transient drying during the Paleocene–Eocene thermal maximum (PETM): analysis of paleosols in the bighorn basin, Wyoming, Palaeogeogr. Palaeocl., 245, 444–461, 2007.
Kurtz, A., Kump, L. R., Arthur, M. A., Zachos, J. C., and Paytan, A.: Early Cenozoic decoupling of the global carbon and sulfur cycles, Paleoceanography, 18, 1090, doi:10.1029/2003PA000908, 2003.
Liu, Z., Pagani, M., Zinniker, D., DeConto, R., Huber, M., Brinkhuis, H., Shah, S. R., Leckie, R. M., and Pearson, A.: Global cooling during the Eocene–Oligocene climate transition, Science, 323, 1187–1190, 2009.
Lourens, L. J., Sluijs, A., Kroon, D., Zachos, J. C., Thomas, E., Röhl, U., Bowles, J., and Raffi, I.: Astronomical pacing of late Palaeocene to early Eocene global warming events, Nature, 435,





CPD
6, 1701–1731, 2010



1083–1087, 2005.
McCarren, H., Thomas, E., Hasegawa, T., Röhl, U., and Zachos, J. C.: Depth dependency of the Paleocene–Eocene carbon isotope excursion: paired benthic and terrestrial biomarker records (Ocean Drilling Program Leg 208, Walvis Ridge), Geochem. Geophy. Geosy., 9, Q10008, doi:10.1029/2008GC002116, 2009.
Pagani, M., Pedentchouk, N., Huber, M., Sluijs, A., Schouten, S., Brinkhuis, H., Sinninghe Damsté, J. S., Dickens, G. R., and The Expedition 302 Scientists: Arctic hydrology during global warming at the Palaeocene-Eocene thermal maximum, Nature, 442, 671–675, 2006.
Panchuk, K., Ridgwell, A., and Kump, L. R.: Sedimentary response to Paleocene–Eocene Thermal Maximum carbon release: a model-data comparison, Geology, 36, 315–318, 2008.
Pearson, P. N., Ditchfield, P. W., Singano, J., Harcourt-Brown, K. G., Nicholas, C. J., Olsson, R. K., Shackleton, N. J., and Hall, M. A.: Warm tropical sea surface temperatures in the late Cretaceous and Eocene epochs, Nature, 413, 481–487, 2001.
Pearson, P. N., van Dongen, B. E., Nicholas, C. J., Pancost, R. D., Schouten, S., Singano, J. M., and Wade, B. S.: Stable warm tropical climate through the Eocene epoch, Geology, 35, 211–214, 2007.
Pross, J. and Brinkhuis, H.: Organic-walled dinoflagellate cysts as paleoenvironmental indicators in the Paleogene; a synopsis of concepts, Palaeont. Z., 79, 53–59, 2005.
Reichart, G.-J., Brinkhuis, H., Huiskamp, F., and Zachariasse, W. J.: Hyperstratification following glacial overturning events in the Northern Arabian Sea, Paleoceanography, 19, PA2013, doi:10.1029/2003PA000900, 2004.
Richter, T. O., Van der Gast, S., Koster, R., Vaars, A., Gieles, R., De Stigter, H. C., De Haas, H., and Van Weering, T. C. E.: The avaatech XRF core scanner: technical description and applications to NE Atlantic sediments, in: New Techniques in Sediments Core Analysis, edited by: Rothwell, R. G., Geological Society London, Special Publication, London, 39–51, 2006.
Robert, C. and Kennett, J. P.: Antarctic subtropical humid episode at the Paleocene–Eocene boundary: clay mineral evidence, Geology, 22, 211–214, 1994.
Röhl, U. and Abrams, L. J.: High-resolution, downhole and non-destructive core measurements from Sites 999 and 1001 in the Caribbean Sea: application to the Late Paleocene Thermal Maximum, in: Proceedings of the Ocean Drilling Program (ODP), Scientific Results 165, Ocean Drilling Program, College Station, TX, 191–203, 2000.





CPD
6, 1701–1731, 2010



Röhl, U., Brinkhuis, H., Sluijs, A., and Fuller, M.: On the search for the Paleocene/Eocene Boundary in the Southern Ocean: exploring ODP leg 189 holes 1171D and 1172D, Tasman Sea, in: The Cenozoic Southern Ocean: Tectonics, Sesimentation, and Climate Change Between Australia and Antarctica. Geophysical Monograph Series 151, edited by: Exon, N. F., Malone, M., and Kennett, J. P., 113–125, 2004.

Röhl, U., Westerhold, T., Monechi, S., Thomas, E., Zachos, J. C., and Donner, B.: The third and final early Eocene Thermal Maximum: characteristics, timing, and mechanisms of the "X" event, Geological Society of America Annual Meeting, Abstr., 37(7), 264, 2005,

Röhl, U., Westerhold, T., Bralower, T. J., and Zachos, J. C.: On the duration of the Paleocene–Eocene Thermal Maximum (PETM), Geochem. Geophy. Geosy., 8, Q12002, doi:10.1029/2007GC001784, 2007.

Schouten, S., Hopmans, E. C., Schefuß, E., and Sinninghe Damsté, J. S.: Distributional variations in marine crenarchaeotal membrane lipids: a new tool for reconstructing ancient sea water temperatures?, Earth Planet. Sc. Lett., 204, 265–274, 2002.

Schouten, S., Huguet, C., Hopmans, E. C., Kienhuis, M. V. M., and Sinninghe Damsté, J. S.: Analytical methodology for $TEX_{86}$ Paleothermometry by high-performance liquid chromatography/atmospheric pressure chemical ionization-mass spectrometry, Anal. Chem., 79, 2940–2944, 2007a.

Schouten, S., Woltering, M., Rijpstra, W. I. C., Sluijs, A., Brinkhuis, H., and Sinninghe Damsté, J. S.: The Paleocene–Eocene carbon isotope excursion in higher plant organic matter: differential fractionation of angiosperms and conifers in the Arctic, Earth Planet. Sc. Lett., 258, 581–592, 2007b.

Schrag, D. P., dePaolo, D. J., and Richter, F. M.: Reconstructing past sea surface temperatures: correcting for diagenesis of bulk marine carbonate, Geochim. Cosmochim. Ac., 59, 2265–2278, 1995.

Shellito, C. J., Sloan, L. C., and Huber, M.: Climate model sensitivity to atmospheric $CO_2$ levels in the Early-Middle Paleogene, Palaeogeogr. Palaeocl., 193, 113–123, 2003.

Shipboard Scientific Party, X. : Site 1172, in: Proceedings of the Ocean Drilling Program, Initial Reports, 189, edited by: Exon, N. F., Kennett, J. P., and Malone, M., Ocean Drilling Program, College Station, TX, 1–149, 2001.

Siringan, F. P., Azanza, R. V., Macalalad, N. J. H., Zamora, P. B., and Sta. Maria, M. Y. Y.: Temporal changes in the cyst densities of Pyrodinium bahamense var. compressum and other dinoflagellates in Manila Bay, Philippines, Harmful Algae, 7, 523–531, 2008.





CPD
6, 1701–1731, 2010



Sluijs, A., Brinkhuis, H., Stickley, C. E., Warnaar, J., Williams, G. L., and Fuller, M.: Dinoflagellate cysts from the Eocene/Oligocene transition in the Southern Ocean; results from ODP Leg 189., in: Proceedings Ocean Drilling Program, Scientific Results 189, edited by: Exon, N. F., Kennett, J. P., and Malone, M. J., College Station, TX, 1–42, 2003.

Sluijs, A., Pross, J., and Brinkhuis, H.: From greenhouse to icehouse; organic-walled dinoflagellate cysts as paleoenvironmental indicators in the Paleogene, Earth-Sci. Rev., 68, 281–315, 2005.

Sluijs, A., Schouten, S., Pagani, M., Woltering, M., Brinkhuis, H., Sinninghe Damsté, J. S., Dickens, G. R., Huber, M., Reichart, G.-J., Stein, R., Matthiessen, J., Lourens, L. J., Pedentchouk, N., Backman, J., Moran, K., and The Expedition 302 Scientists: Subtropical Arctic Ocean temperatures during the Palaeocene/Eocene Thermal Maximum, Nature, 441, 610–613, 2006.

Sluijs, A., Bowen, G. J., Brinkhuis, H., Lourens, L. J., and Thomas, E.: The Palaeocene-Eocene thermal maximum super greenhouse: biotic and geochemical signatures, age models and mechanisms of global change, in: Deep Time Perspectives on Climate Change: Marrying the Signal from Computer Models and Biological Proxies, edited by: Williams, M., Haywood, A. M., Gregory, F. J., and Schmidt, D. N., The Micropalaeontological Society, Special Publications, The Geological Society, London, 323–347, 2007a.

Sluijs, A., Brinkhuis, H., Schouten, S., Bohaty, S. M., John, C. M., Zachos, J. C., Reichart, G.-J., Sinninghe Damsté, J. S., Crouch, E. M., and Dickens, G. R.: Environmental precursors to light carbon input at the Paleocene/Eocene boundary, Nature, 450, 1218–1221, 2007b.

Sluijs, A., Brinkhuis, H., Crouch, E. M., John, C. M., Handley, L., Munsterman, D., Bohaty, S., M., Zachos, J. C., Reichart, G.-J., Schouten, S., Pancost, R. D., Sinninghe Damsté, J. S., Welters, N. L. D., Lotter, A. F., and Dickens, G. R.: Eustatic variations during the Paleocene–Eocene greenhouse world, Paleoceanography, 23, PA4216, doi:10.1029/2008PA001615, 2008a.

Sluijs, A., Röhl, U., Schouten, S., Brumsack, H.-J., Sangiorgi, F., Sinninghe Damsté, J. S., and Brinkhuis, H.: Arctic late Paleocene–early Eocene paleoenvironments with special emphasis on the Paleocene–Eocene Thermal Maximum (Lomonosov Ridge, Integrated Ocean Drilling Program Expedition 302), Paleoceanography, 23, PA1S11, doi:10.1029/2007PA001495, 2008b.

Sluijs, A. and Brinkhuis, H.: A dynamic climate and ecosystem state during the Paleocene–Eocene Thermal Maximum: inferences from dinoflagellate cyst assemblages on the New





CPD
6, 1701–1731, 2010



Jersey Shelf, Biogeosciences, 6, 1755–1781, doi:10.5194/bg-6-1755-2009, 2009.
Sluijs, A., Brinkhuis, H., Williams, G. L., and Fensome, R. A.: Taxonomic revision of some Cretaceous-Cenozoic spiny organic-walled, peridinioid dinoflagellate cysts, Rev. Palaeobot. Palyno., 154, 34–53, 2009a.
Sluijs, A., Schouten, S., Donders, T. H., Schoon, P. L., Röhl, U., Reichart, G.-J., Sangiorgi, F., Kim, J.-H., Damsté, J. S. S., and Brinkhuis, H.: Warm and wet Arctic conditions during Eocene thermal maximum 2, Nat. Geosci., 2, 777–780, 2009b.
Speijer, R. P. and Wagner, T.: Sea-level changes and black shales associated with the late Paleocene Thermal Maximum: organic-geochemical and micropaleontologic evidence from the Southern Tethyan margin (Egypt-Israel), Geol. S. Am. S., 356, 533–549, 2002.
Stap, L., Lourens, L. J., Thomas, E., Sluijs, A., Bohaty, S. M., and Zachos, J. C.: High-resolution deep-sea carbon and oxygen isotope records of Eocene Thermal Maximum 2 and $H_2$, Geology, 38, 607–610, 2010.
Steurbaut, E., Magioncalda, R., Dupuis, C., Van Simaeys, S., Roche, E., and Roche, M.: Palynology, paleoenvironments, and organic carbon isotope evolution in lagoonal Paleocene–Eocene boundary settings in North Belgium, in: Causes and consequences of Globally Warm Climates in the Early Paleogene, Geological Society of America Special Paper 369, edited by: Wing, S. L., Gingerich, P., Schmitz, B., and Thomas, E., Geological Society of America, Boulder, Colorado, 291–317, 2003.
Stickley, C. E., Brinkhuis, H., McGonigal, K., Chaproniere, G., Fuller, M., Kelly, D. C., Nürnberg, D., Pfuhl, H. A., Schellenberg, S. A., Schoenfeld, J., Suzuki, N., Touchard, Y., Wei, W., Williams, G. L., Lara, J. and Stant, S. A.: Late Cretaceous–Quaternary biomagnetostratigraphy of ODP Sites 1168, 1170, 1171, and 1172, Tasmanian Gateway, in: Proceedings of the Ocean Drilling Program, Scientific Results, 189, edited by: Exon, N. F., Kennett, J. P., and Malone, M. J., College Station, TX, 1–57, 2004.
Stockmarr, J.: Tablets with spores used in absolute pollen analysis, Pollen Spores, 13, 615–621, 1972.
Svensen, H., Planke, S., Malthe-Sørensen, A., Jamtveit, B., Myklebust, R., Eidem, T. R., and Rey, S. S.: Release of methane from a volcanic basin as a mechanism for initial Eocene global warming, Nature, 429, 542–545, 2004.
Thomas, D. J., Zachos, J. C., Bralower, T. J., Thomas, E., and Bohaty, S.: Warming the fuel for the fire: Evidence for the thermal dissociation of methane hydrate during the Paleocene–Eocene thermal maximum, Geology, 30, 1067–1070, 2002.





CPD
6, 1701–1731, 2010



Thomas, E. and Shackleton, N. J.: The Palaeocene-Eocene benthic foraminiferal extinction and stable isotope anomalies., in: Correlation of the Early Paleogene in Northwestern Europe, Geological Society London Special Publication, 101, edited by: Knox, R. W. O. B., Corfield, R. M., and Dunay, R. E., Geological Society of London, London, UK, 401–441, 1996.

Tjallingii, R., Röhl, U., Kölling, M., and Bickert, T.: Influence of the water content on X-ray fluorescence core scanning measurements in soft marine sediments, Geochem. Geophy. Geosy., 8, Q02004, doi:10.1029/2006GC001393, 2007.

Tripati, A. and Elderfield, H.: Deep-sea temperature and circulation changes at the Paleocene–Eocene Thermal Maximum, Science, 308, 1894–1898, 2005.

Uchikawa, J. and Zeebe, R. E.: Examining possible effects of seawater pH decline on foraminiferal stable isotopes during the Paleocene–Eocene Thermal Maximum, Paleoceanography, 25, PA2216, doi:10.1029/2009PA001864, 2010.

Villanoy, C., Corralet, R. A., Jacinto, G. S., Cuaresma, N., and Crisostomo, R.: Towards the development of a cyst-based model for Pyrodinium red tides in Manila Bay, in: Harmful Toxic Algal Blooms, edited by: Yasumoto, T., Oshima, Y., and Fukuyo, Y., IOC of UNESCO, Paris, 189–192, 1996.

Villanoy, C. L., Azanza, R. V., Altemerano, A., and Casil, A. L.: Attempts to model the bloom dynamics of Pyrodinium, a tropical toxic dinoflagellate, Harmful Algae, 5, 156–183, 2006.

Wall, D., Dale, B., Lohmann, G. P., and Smith, W. K.: The environmental and climatic distribution of dinoflagellate cysts in modern marine sediments from regions in the North and South Atlantic Oceans and adjacent seas, Mar. Micropaleontol., 2, 121–200, 1977.

Warnaar, J., Bijl, P. K., Huber, M., Sloan, L., Brinkhuis, H., Röhl, U., Sriver, R., and Visscher, H.: Orbitally forced climate changes in the Tasman sector during the Middle Eocene, Palaeogeogr. Palaeocl., 280, 361–370, 2009.

Weijers, J. W. H., Schouten, S., Spaargaren, O. C., and Sinninghe Damsté, J. S.: Occurrence and distribution of tetraether membrane lipids in soils: implications for the use of the $TEX_{86}$ proxy and the BIT index, Org. Geochem., 37, 1680–1693, 2006.

Weijers, J. W. H., Schouten, S., Sluijs, A., Brinkhuis, H., and Sinninghe Damsté, J. S.: Warm arctic continents during the Palaeocene-Eocene Thermal Maximum, Earth Planet. Sc. Lett., 261, 230–238, 2007.

Westerhold, T., Röhl, U., Laskar, J., Raffi, I., Bowles, J., Lourens, L. J., and Zachos, J. C.: On the duration of Magnetochrons C24r and C25n, and the timing of early Eocene global warming





CPD
6, 1701–1731, 2010



events: implications from the ODP Leg 208 Walvis Ridge depth transect, Paleoceanography, 22, PA2201, doi:10.1029/2006PA001322, 2007.
Wing, S. L., Harrington, G. J., Smith, F. A., Bloch, J. I., Boyer, D. M., and Freeman, K. H.: Transient floral change and rapid global warming at the Paleocene–Eocene boundary, Science, 310, 993–996, 2005.
Wrenn, J. H. and Beckmann, S. W.: Maceral, total organic carbon, and palynological analyses of Ross Ice Shelf Project site J9 cores, Science, 216, 187–189, 1982.
Zachos, J., Pagani, M., Sloan, L., Thomas, E., and Billups, K.: Trends, rhythms, and aberrations in global climate 65 Myr to present, Science, 292, 686–693, 2001.
Zachos, J. C., Lohmann, K. C., Walker, J. C. G., and Wise, S. W.: Abrupt climate change and transient climates during the Palaeogene: a marine perspective, J. Geol., 101, 191–213, 1993.
Zachos, J. C., Wara, M. W., Bohaty, S., Delaney, M. L., Petrizzo, M. R., Brill, A., Bralower, T. J., and Premoli Silva, I.: A transient rise in tropical sea surface temperature during the Paleocene–Eocene Thermal Maximum, Science, 302, 1551–1554, 2003.
Zachos, J. C., Röhl, U., Schellenberg, S. A., Sluijs, A., Hodell, D. A., Kelly, D. C., Thomas, E., Nicolo, M., Raffi, I., Lourens, L. J., McCarren, H., and Kroon, D.: Rapid acidification of the ocean during the Paleocene–Eocene Thermal Maximum, Science, 308, 1611–1615, 2005.
Zachos, J. C., Schouten, S., Bohaty, S., Quattlebaum, T., Sluijs, A., Brinkhuis, H., Gibbs, S., and Bralower, T. J.: Extreme warming of mid-latitude coastal ocean during the Paleocene–Eocene thermal maximum: inferences from $TEX_{86}$ and isotope data, Geology, 34, 737–740, 2006.
Zachos, J. C., Bohaty, S. M., John, C. M., McCarren, H., Kelly, D. C., and Nielsen, T.: The Palaeocene-Eocene carbon isotope excursion: constraints from individual shell planktonic foraminifer records, Philos. T. R. Soc. A, 365, 1829–1842, 2007.
Zeebe, R. E., Zachos, J. C., and Dickens, G. R.: Carbon dioxide forcing alone insufficient to explain Palaeocene-Eocene thermal maximum warming, Nat. Geosci., 2, 576–580, 2009.





CPD
6, 1701–1731, 2010



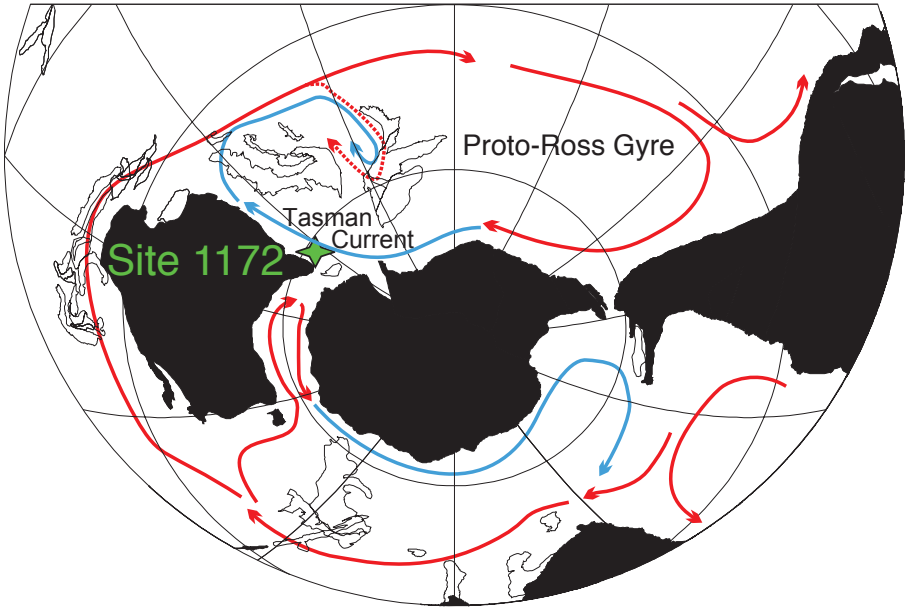


**Fig. 1.** Site location and surface currents. Early Eocene Paleogeographic reconstruction for the Antarctic. Surface circulation (Huber et al., 2004) indicates the Antarctic-derived Tasman Current over the East Tasman Plateau, which is supported by biogeographical data. Paleogeographic chart obtained from the Ocean Drilling Stratigraphic Network (ODSN) and was modified from Bijl et al. (2009). The dashed red arrow around New Zealand indicates potential mixing of low-latitude surface waters (from the East Australian Current) with the Tasman Current.





CPD
6, 1701–1731, 2010



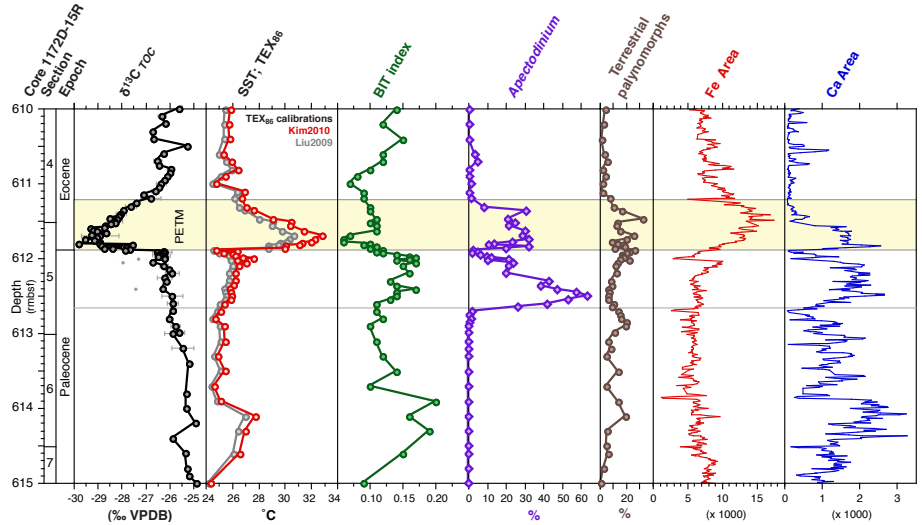


**Fig. 2.** Organic geochemical, palynological and XRF results across the PETM of Site 1172. From left to right: stable carbon isotope ($\delta^{13}$C) values of total organic carbon (TOC) relative to the Vienna Pee Dee Belemnite standard. Error bars reflect duplicate-based standard deviations and three grey data points are considered outliers because duplicate analyses indicated values consistent with surrounding samples; sea surface temperature (SST) based on $TEX_{86}$ following the calibrations KIM2010 (Kim et al., 2010) and LIU2009 (Liu et al., 2009); BIT index; *Apectodinium* percentage of the dinocyst assemblage; abundance of terrestrially derived palynomorphs as a percentage of total palynomorphs; and XRF intensity data for iron and calcium.





CPD
6, 1701–1731, 2010

Southern Ocean PETM warming, hydrology and sea level

A. Sluijs et al.



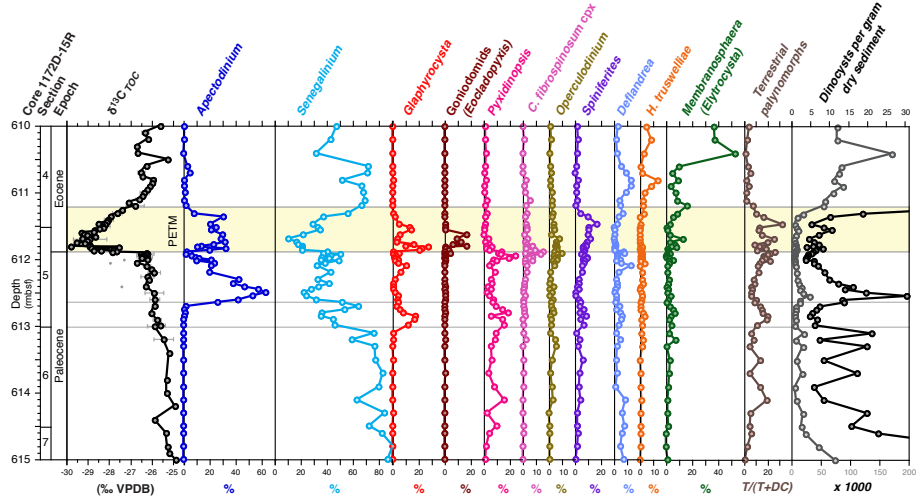


**Fig. 3.** Palynological results across the PETM of Site 1172. Dinocyst abundances are reflected as the percentage of the total dinocyst assemblage and the abundance of terrestrially derived palynomorphs as a percentage of total palynomorph sum. Goniodomids almost exclusively represent *Eocladopyxis peniculatum*. *Membranosphaera* is often referred to as *Elytrocysta* in Southern Ocean literature. Grey and black lines in the absolute quantitative dinocyst abundance panel reflect two different scales for illustration purposes.





CPD
6, 1701–1731, 2010

Southern Ocean PETM warming, hydrology and sea level

A. Sluijs et al.